Received: 9 September 2019 | Revised: 18 November 2019 | Accepted: 8 December 2019

DOI: 10.1002/ardp.201900264

DPhG ARCH PHARM
Archiv der Pharmazie

FULL PAPER

Synthesis and anti-inflammatory effects of novel emodin derivatives bearing azole moieties

Xiaokang Zhu[1] | Qifang Chen[1] | Yujin Yang[2] | Xixi Ai[1] | Si Chen[1] | Yang Song[1]

[1]Key Laboratory of Luminescence and Real-Time Analytical Chemistry (Southwest University), Ministry of Education, College of Pharmaceutical Sciences, Southwest University, Chongqing, China

[2]Research and Development Center, Chongqing Huapont Pharmaceutical Co. Ltd., Chongqing, China

Correspondence
Xiaokang Zhu and Yang Song, Key Laboratory of Luminescence and Real-Time Analytical Chemistry (Southwest University), Ministry of Education, College of Pharmaceutical Sciences, Southwest University, 400716 Chongqing, China.
Email: zxk@swu.edu.cn (X. Z.) and songyangwenrong@hotmail.com (Y. S.)

Funding information
National Natural Science Foundation of China, Grant/Award Number: 21602180; National Experimental Teaching Demonstration Center of Pharmaceutical Sciences, Grant/Award Number: YX2017-CXZD-05

Abstract

Twelve azole derivatives of emodin were designed to possess anti-inflammatory activity and synthesized via a two-step sequence composed of the Williamson ether reaction and *N*-alkylation. The anti-inflammatory properties of these compounds were evaluated in RAW264.7 cells by measuring lipopolysaccharide (LPS)-induced nitric oxide (NO) production. The introduction of imidazole and four carbons into the scaffold of emodin led to the discovery of the potent compound **7e**, which showed the best inhibition of NO production among twelve analogs. In our experiential setting, the IC_{50} of compound **7e** in NO production is 1.35 μM, which is lower than that of indomethacin. Mechanically, compound **7e** effectively inhibited the protein and messenger RNA expressions of cyclooxygenase-2 and inducible NO synthase, as well as that of the proinflammatory cytokine interleukin-6, and the cytokines interleukin-1β and tumor necrosis factor-α in the LPS-stimulated RAW 264.7 macrophages. Compound **7e** exerted inhibitory effects on the nuclear factor κB pathway by reducing the LPS-induced phosphorylation of the inhibitor of NF-κB and the nuclear translation of p-p65. These results suggest the potential of compound **7e** in improving inflammatory conditions and diseases.

KEYWORDS
anti-inflammatory activity, emodin derivatives, lipopolysaccharide, NF-κB pathway

1 | INTRODUCTION

Emodin is an anthraquinone derivative that was originally isolated from the traditional Chinese herbs *Polygonum cuspidatum* and *Rheum rhaponticum*, which have been used in China as a purging drug for thousands of years. Previous studies have shown that emodin possesses a wide spectrum of pharmacological properties, such as antimicrobial, anti-inflammatory, antioxidant, and anticancer activities.[1] The majority of existing studies have focused on the anti-inflammatory properties of this compound.[2–4] For instance, Li et al.[3] demonstrated that emodin attenuated titanium particle-induced osteolysis and osteoclastogenesis through the suppression of the nuclear factor-κB (NF-κB) signal pathway. In addition, Liang et al.[4] showed that emodin attenuated lipopolysaccharide (LPS)-induced apoptosis and inflammation through the inhibition of the Notch and NF-κB pathway.

There is continued interest in the synthesis of new emodin derivatives with improved biological activity and reduced toxicity. Wang et al. synthesized a series of novel quaternary ammonium salts of emodin (compound **1**) with better in vitro anticancer activities than emodin.[5,6] Koerner et al.[7] designed a series of emodin derivatives (compound **2**) which may act as ATP-citrate lyase inhibitors. A structure–activity relationship (SAR) study indicated that the two OH groups adjacent to the 9-carbonyl group may be critical for on-target activity. For instance, Wu et al.[8] developed a series of novel 1,4-pentadien-3-one derivatives (compounds **3** and **4**) bearing an emodin moiety with protective activity against the tobacco mosaic virus. Another group showed a series of emodin derivatives bearing polyamine side chains (compound **2**) as effective inhibitors of potent p-glycoprotein.[9] We previously reported that the introduction of an alkyl substituent on the anthraquinone ring of emodin could improve the lipophilicity and enhance the antibacterial and hypoglycemic activities of these compounds.[10,11] Figure 1 shows some structures of emodin derivatives which have been investigated.

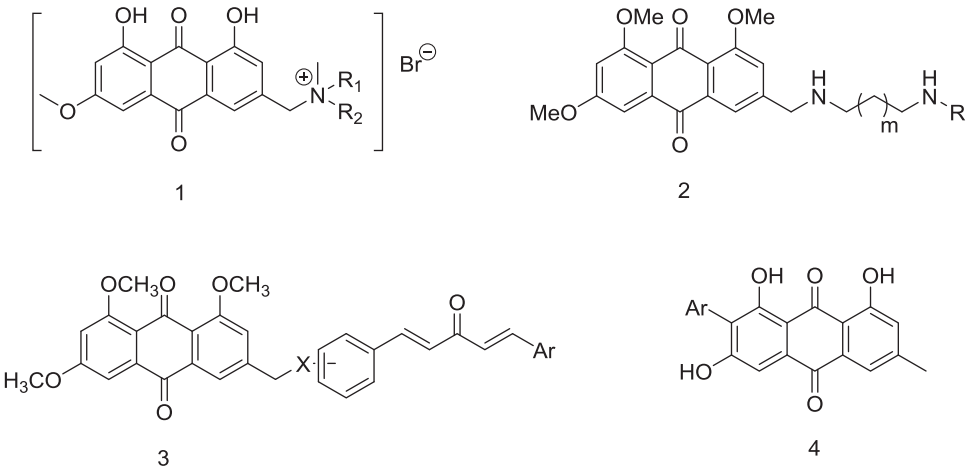

FIGURE 1 Emodin derivatives with improved biocompatibility and activities

NF-κB signal plays a crucial role in inflammation and immune responses.[12] The NF-κB dimers are sequestered in the cytoplasm by a family of inhibitors, IκB, which mask the nuclear localization signals of NF-κB proteins and keep them sequestered in an inactive state in the cytoplasm.[13] Activation of NF-κB by nuclear translocation plays a role in inflammation through the induction of transcription of several proinflammatory genes.[14] Thus, dysregulated NF-κB/IκB signaling contributes to the pathogenic processes of various inflammatory diseases, such as rheumatoid arthritis, inflammatory bowel disease, multiple sclerosis, atherosclerosis, systemic lupus erythematosus, type I diabetes, chronic obstructive, pulmonary disease, and asthma.[15] Therefore, it is of great value to design and synthesize novel chemical entities, which are able to block the NF-κB signaling pathway.[16–19]

Azole-based compounds possess good anti-inflammatory activity with improved safety profiles.[20,21] We designed a series of novel emodin azole derivatives by merging the triazole/imidazole scaffold with emodin nucleus using the hybrid approach and expected to gain improved bioavailability, and additive or synergistic actions in anti-inflammatory activity.[22] The synthesized compounds were in vitro assayed for anti-inflammatory activity by measuring LPS-induced NO production. Meanwhile, the selected compound was assayed for the inhibition of the inflammatory cytokines and the detailed molecular mechanism was discussed.

2 | RESULTS AND DISCUSSION

2.1 | Chemistry

The synthesis of compounds **6a–f** and **7a–f** is described in Scheme 1. Emodin was treated with dibromoalkanes that possessed two to six carbons, tetrabutylammonium bromide (TBAB), and K_2CO_3 in

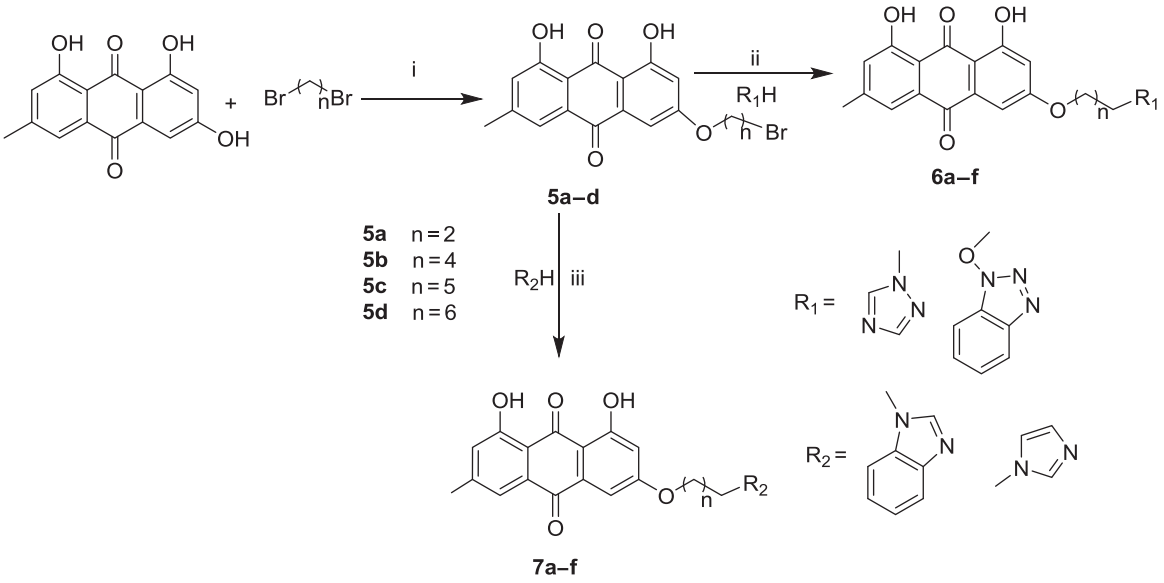

SCHEME 1 Synthetic route of emodin azole derivatives. Reagents and conditions: (i) TBAB, K_2CO_3, DMF, 6 hr, 75°C, 48–65%; (ii) DMSO, K_2CO_3, 8 hr, r.t. 16–45%; (iii) NaH, THF, 3 hr, 75°C, 20–50%. DMF, dimethylformamide; DMSO, dimethyl sulfoxide; TBAB, tetra-*n*-butylammonium bromide; THF, tetrahydrofuran

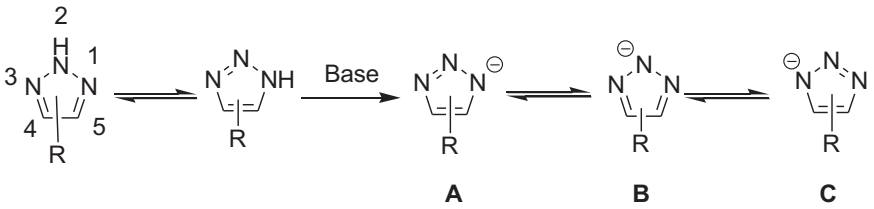

FIGURE 2 The tautomer and resonance structures of triazole

dimethylformamide (DMF). The corresponding bromo-substituted compounds **5a–d** were afforded in the 48–68% yield. In the preparation of **5a–d**, both the reaction temperature and the ratio of emodin to dibromoalkane are critical parameters. When the ratio of emodin to dibromoalkane was more than 1:1.2, the desired monobromoalkane-substituted emodin was obtained, due to the different activities of the three hydroxyl groups within emodin. The other two hydroxyl groups are inert due to the conformation of the intramolecular hydrogen bond. TBAB was required to transfer K_2CO_3 from the aqueous phase to the organic phase in the ether solution.

Compounds **5a–d** were then treated with a variety of substituent triazoles, in the presence of K_2CO_3 and (dimethyl sulfoxide) DMSO, to afford compounds **6a–f** (16–50% yield). Alternatively, the treatment of **5a–d** with a variety of imidazoles and benzimidazoles, in the presence of NaH in tetrahydrofuran (THF), provided the target compounds **7a–f** (20–50% yield). In the preparation of the **6a–f**, emodin in DMSO was dropped into the triazole derivatives with K_2CO_3 in DMSO at room temperature. In the presence of the base, there are two tautomer and three resonance structures of triazole (Figure 2).[23,24] The resonance structures **A** and **C** are dynamically stable, existing at low temperature in weak alkali conditions. As imidazole has a lower acidity than triazole, the strong base NaH was needed in the preparation of the **7a–f**.

The synthesis of 1-(4-phenoxybutyl)-1*H*-imidazole **9a**, which could be compared to emodin imidazole was also accomplished, as shown in Scheme 2. To the best of our knowledge, compounds **6a–f** and **7a–f** have not been reported before. The molecular structures of all new compounds were characterized by ^{1}H NMR (nuclear magnetic resonance), ^{13}C NMR, and high-resolution mass spectrometry.

2.2 | Evaluation of anti-inflammatory activity

2.2.1 | Inhibition of NO production in LPS-stimulated macrophages

LPS-induced excessive NO generation occurs at different stages of inflammatory conditions.[25] Therefore, pharmacological interference with NO production presents promising strategies for therapeutic intervention in inflammatory disorders. Hence, 12 target compounds (**6a–f** and **7a–f**), together with emodin and indomethacin as controls, were evaluated for their inhibition efficiency of NO production in LPS-stimulated RAW 264.7 macrophages (Table 1). A cell-counting kit-8 assay was performed to rule out the possibility that the inhibition of inflammatory response was caused by their cytotoxicity. RAW 264.7 macrophages were treated with individual compounds at 20 μM, with or without LPS, for 24 hr, and the results indicated imperceptible cytotoxicity. Preliminary screening showed that the majority of emodin derivatives exhibited stronger inhibitory activities against LPS-induced NO production in RAW 264.7 macrophages as well as emodin. Among them, compound **7e** (IC_{50} = 1.35 μM) showed better activity than both emodin (IC_{50} = 4.80 μM) and the positive control indomethacin (IC_{50} = 12.6 μM).

SAR analysis revealed that the emodin ring plays an important role in the inhibition of NO production because IC_{50} values of **9a** (>20 μM) for NO inhibition was bigger than that of other emodin azole derivatives. The NO inhibition increased in the compounds with imidazole substitute (**7d–f**) compared with a triazole, indicating that the imidazole moiety is crucial. Surprisingly, compound **7a–c** with a benzene ring on the azole as a substitution group showed no contribution to NO inhibition, compared with compound **7d–f**. The length of the alkyl chain between the two heterocyclic moieties plays an important role in the inhibition of NO production in vitro. The values of IC_{50} of NO inhibition of different compounds are listed in Table 1. NO inhibition differs with different carbon alkyl chain linkers in the emodin azole derivatives. In general, the emodin azole derivatives with four-carbon alkyl chain linkers, such as compounds **6b**, **7b**, and **7e**, showed the strongest inhibitory activities, with compound **7e** having the best potential. Almost all the emodin azole derivatives have better NO inhibition than indomethacin. For this reason, compound **7e** was selected as a candidate for further studies on the mechanism of anti-inflammatory activity.

2.2.2 | Compound 7e inhibits the induction of iNOS and COX-2

Next, we explored the molecular mechanism of compound **7e** in NO inhibition and anti-inflammatory activity. In the activated

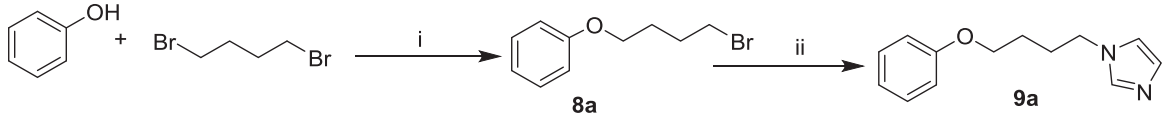

SCHEME 2 Synthetic route of 1-(4-phenoxybutyl)-1*H*-imidazole. Reagents and conditions: (i) TBAB, K_2CO_3, DMF, 24 hr, 75°C, 47%; (ii) NaH, THF, 1*H*-imidazole, 3 hr, 60°C, 74%. DMF, dimethylformamide; TBAB, tetra-*n*-butylammonium bromide; THF, tetrahydrofuran

TABLE 1 Chemical structures of the target compounds and their inhibition of NO production in lipopolysaccharide-stimulated RAW 264.7 cells

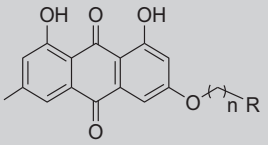

Compound	*n*	R	ClgP[a]	Inhibition of NO (IC_{50} [μM])
6a	2	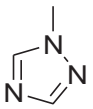	3.28	4.24
6b	4	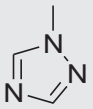	3.81	2.24
6c	6	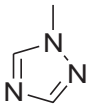	4.87	5.58
6d	4	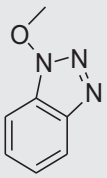	5.76	15.83
6e	5	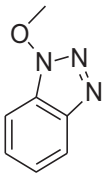	6.29	6.11
6f	6	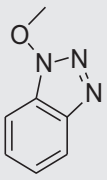	6.82	11.08
7a	2	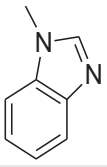	5.48	3.31
7b	4	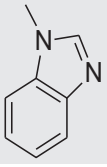	6.13	2.44
7c	6	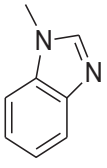	7.19	7.23
7d	2	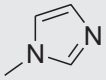	3.88	9.83
7e	4	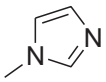	4.54	1.35
7f	6	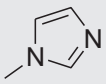	5.60	3.32
9a			2.41	>20
Emodin			–	4.80
Indomethacin			–	12.61

[a]Calculated using ChemDraw ultra 8.0.

(Continues)

macrophages, the transcriptionally expressed inducible NO synthase (iNOS) is responsible for the prolonged and profound production of NO.[26] As the overproduction of NO is the result of high levels of iNOS expression, we studied the ability of **7e** and indomethacin to modulate LPS-induced iNOS expression. Cyclooxygenase-2 (COX-2) is the predominant COX isoform present at sites of inflammation and produces prostaglandins that cause swelling and pain.[27] Both COX-1 and COX-2 are the targets of nonsteroidal anti-inflammatory drugs (NSAIDs),[28] however, COX-2 is readily inducible and seems to be more important than COX-1 in various pathological functions. Thus, we examined the effect of **7e** on iNOS and COX-2 expression. After plating and 24 hr of growth, RAW 264.7 macrophages were treated with **7e** or indomethacin, in the presence or absence of 1 μg/ml LPS, for 6 hr. The cell lysates were electrophoresed, and the expression levels of iNOS and COX-2 were detected with specific antibodies. As shown in Figure 3, LPS increased the expression of iNOS and COX-2 compared with the control group significantly ($p < 0.001$). However, this expression was markedly attenuated in RAW 264.7 macrophages that were pretreated with **7e**. Correlating with NO measurement, indomethacin also exhibited significant inhibition of iNOS expression.

Similar patterns were observed for the effect of **7e** on LPS-induced iNOS and COX-2 mRNA (messenger RNA) expression. After treatment with **7e** or indomethacin at 2.5 μM for 1 hr and then treatment with LPS for 6 hr, total RNA was prepared from RAW 264.7 cells and qPCR was performed for the iNOS and COX-2 genes. These findings indicate that treatment with **7e** significantly attenuated the LPS-stimulated induction of iNOS and COX-2 expression through transcriptional inhibition.

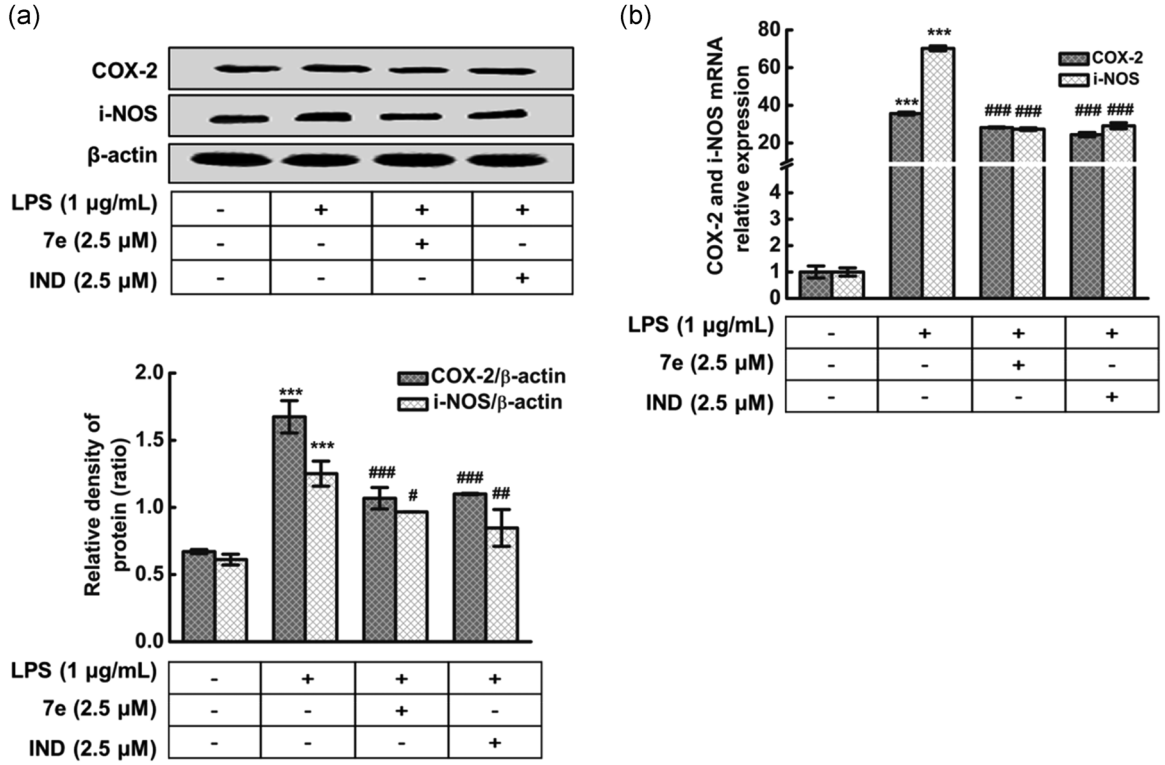

FIGURE 3 Effects of **7e** and indomethacin on LPS-induced iNOS and COX-2 protein (a) and mRNA (b) expression in RAW 264.7 macrophages. β-Actin was used as an internal control for Western blot analysis and reverse-transcription polymerase chain reaction assay. (a) Western blot analysis for the COX-2 and iNOS protein levels in LPS-induced RAW 264.7 macrophages; densitometry analyses are presented as the relative ratios of iNOS/control and COX-2/control. (b) Effects of **7e** and indomethacin on LPS-induced iNOS and COX-2 mRNA expression. The mRNA levels ($2^{-\Delta C_t}$) of each gene were determined by quantitative real-time PCR. The bar graphs show the mean ± SEM of three independent experiments. The bar graphs show the mean ± SEM of three independent experiments: $^{###}p < 0.001$ for the LPS group compared with the control group; $^{***}p < 0.001$ compared with the LPS group. COX-2, cyclooxygenase-2; iNOS, inducible NO synthase; LPS, lipopolysaccharide; mRNA, messenger RNA; SEM, standard error of the means

2.2.3 | Compound 7e inhibits the release of inflammatory cytokines

Interleukin-6 (IL-6), IL-1β, and tumor necrosis factor-α (TNF-α) are early-secreted proinflammatory cytokines. Elevated levels in the expression of these cytokines are observed in a variety of acute and chronic inflammatory diseases. We determined the effects of **7e** and indomethacin IL-6, IL-1β, and TNF-α in LPS-stimulated cells. RAW 264.7 cells were incubated with **7e** or indomethacin for 1 hr and then treated with LPS (1 μg/ml) for 6 hr. The cell lysates were electrophoresed, and the expression levels of IL-6, IL-1β, and TNF-α were detected with specific antibodies. As shown in Figure 4, the protein levels of IL-6, IL-1β, and TNF-α were significantly downregulated in the presence of **7e** after stimulation with LPS (1 μg/ml) with a concentration of 2.5 mM. The protein levels and mRNA level of TNF-α, IL-1β, and IL-6 were increased after being incubated with LPS compared with the vehicle group, whereas the increase of IL-1β and TNF-α, IL-6 level was inhibited by **7e** and indomethacin pretreatment. Similar results were obtained using the enzyme-linked immunosorbent assay (ELISA) kit of the proinflammatory cytokines.

2.2.4 | Compound 7e inhibits NF-κB activity

The activation of the NF-κB signaling pathway will release the cytokine and lead to the overproduction of NO and iNOS, hence, the inhibition of NF-κB in RAW 264.7 cells stimulated by LPS was examined. IκB plays a crucial role in the regulation of NF-κB activation, as the release of activated NF-κB is mediated by the phosphorylation and degradation of IκB. As shown in Figure 5a, LPS stimulation caused an increase in the inhibitor of NF-κB (IκBα) phosphorylation. Compound **7e** and indomethacin significantly decrease the IκBα phosphorylation. Activated NF-κB can enter the nucleus and initiate transcription, and the cytokine will be released. To prove whether the anti-inflammatory activity of compound **7e** is through inhibition of the NF-κB signaling pathway, we examined the effect of **7e** and indomethacin on the nuclear translocation of NF-κB induced by LPS. In Figure 5b, nuclear NF-κB increased obviously in RAW 264.7 cells after LPS stimulation for 6 hr, whereas pretreatment with **7e** blocked the LPS-induced nuclear translocation of NF-κB. Moreover, immunostaining was performed to confirm the effect of compound **7e** on NF-κB cellular distribution in RAW264.7 macrophages. We found that **7e** and indomethacin inhibited the

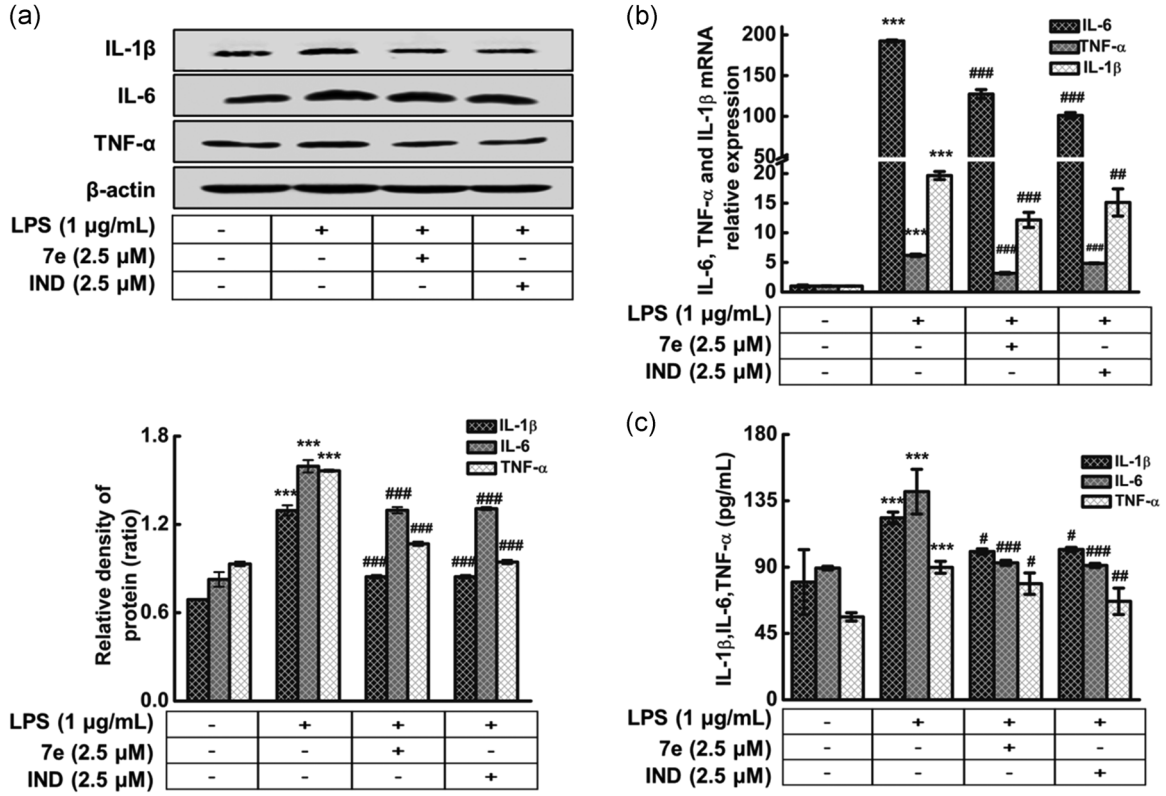

FIGURE 4 Effects of **7e** and indomethacin on LPS-induced IL-6, IL-1β, and TNF-α protein expression in RAW 264.7 macrophages. (a) Western blot analysis for the IL-6, IL-1β, and TNF-α in LPS-induced RAW 264.7 macrophages. Densitometry analyses are presented as the relative ratios of IL-6, IL-1β, and TNF-α to control. (b) Effects of **7e** and indomethacin on LPS-induced IL-6, IL-1β, and TNF-α mRNA expression. The mRNA levels ($2^{-\Delta Ct}$) of each gene were determined by quantitative real-time polymerase chain reaction. The bar graphs show the mean ± SEM of three independent experiments. C, Effects of **7e** and indomethacin on LPS-induced IL-6, IL-1β, and TNF-α expression for enzyme-linked immunosorbent assay. The bar graphs show the mean ± SEM of three independent experiments: $^{###}p < 0.001$ for the LPS group compared with the control group; $^{***}p < 0.001$ compared with the LPS group. IL, interleukin; LPS, lipopolysaccharide; mRNA, messenger RNA; SEM, standard error of the means, TNF-α, tumor necrosis factor-α

LPS-induced nuclear distribution of p-p65 in RAW 264.7 cells in Figure 5c, which indicates that the compound **7e** can suppress the inflammatory activity by inhibiting the NF-κB signaling pathway.

3 | CONCLUSION

In conclusion, 12 emodin derivatives were designed, synthesized and evaluated for anti-inflammatory activity. Biological studies showed that these derivatives detected anti-inflammatory activity by the inhibition of the production of NO stimulated by LPS in RAW 264.7 cells. SAR studies indicated that the anthraquinone ring is essential to the anti-inflammatory activity. Imidazole is a better substitute group than triazole with regard to the inhibition of NO release. Furthermore, the length of the carbon chain influenced the inhibition of NO release. For instance, compound **6b** with four-carbon alkyl chain linkers showed stronger inhibitory activities than **6a** and **6c**. Compound **7e** exhibited the greatest inhibition of NO release. Mechanically, compound **7e** inhibits iNOS and COX-2 expression at the protein level and mRNA level. In the study, we also demonstrated that **7e** decreases the expression of inflammatory cytokines IL-6, IL-1β, and TNF-α and inhibits the LPS-induced activation of NF-κB. It can be deduced that **7e** inhibited LPS-induced expression of inflammatory mediators in RAW 264.7 cells through the blockage of NF-κB pathways. The results obtained in this study may lead to a better understanding of SARs and chemical modifications that enhance the bioactivity of emodin, with the aim of improving its anti-inflammatory activity.

4 | EXPERIMENTAL

4.1 | Chemistry

4.1.1 | General

Melting points were recorded using a digital melting point meter (Tianjin, China) and are uncorrected. ^{1}H NMR spectra were determined at 400/600 MHz using a Bruker AM-400/600 spectrophotometer using tetramethylsilane as an internal reference and ^{13}C NMR spectra were determined at 100/125 MHz using a Bruker 100/125 MHz NMR spectrometer. Mass spectra were measured by the electrospray ionization (ESI) method on an Agilent 6510 Q-TOF mass spectrometer.

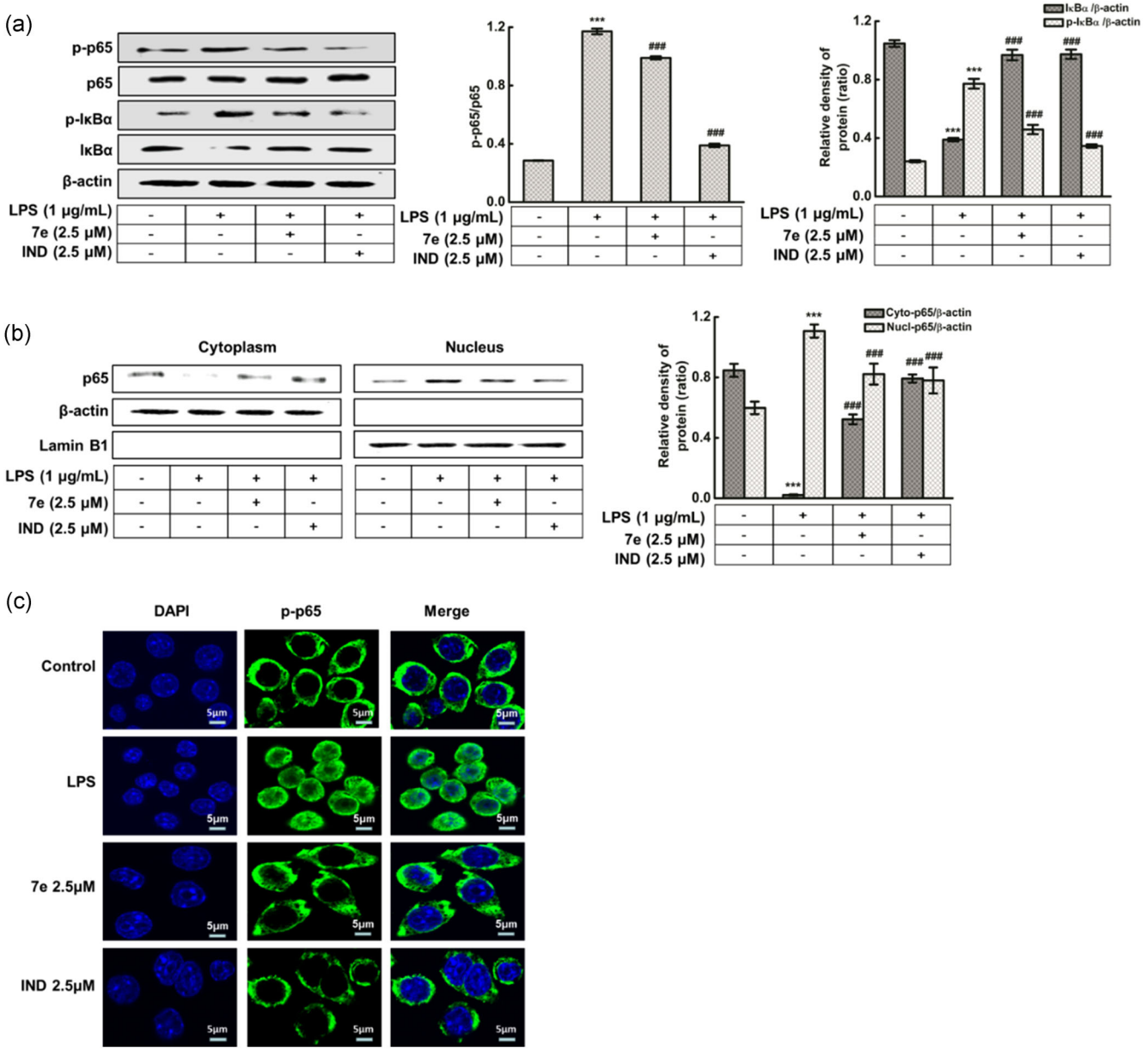

FIGURE 5 Effects of **7e** and indomethacin on LPS-induced NF-κB signaling pathway. (a) The protein level of NF-κB and phospho-IκBα were analyzed by Western blot analysis, Densitometry analyses are presented as the relative ratios of NF-κB/control and p-IκBα/control. (b) The nuclear part and the cytoplasm part of NF-κB were detected by Western blot analysis. Lamin B was used as a loading control in the nuclear part. However, β-actin was used as a loading control in the cytoplasm. (c) Nuclear localization of NF-κB of RAW264.7 cells was assayed by immunostaining with p-p65 (Green), and counterstained with DAPI (blue), the images were obtained by confocal microscopy. The bar graphs show the mean ± SEM of three independent experiments: $^{###}p < 0.001$ for the LPS group compared with the control group; $^{***}p < 0.001$ compared with the LPS group. DAPI, 4′,6-diamidino-2-phenylindole; IκBα, inhibitor of NF-κB; LPS, lipopolysaccharide; NF-κB, nuclear factor-κB; SEM, standard error of the means

The InChI codes of the investigated compounds together with some biological activity data are provided as Supporting Information.

4.1.2 | General procedures for the preparation of 5a–d

To a solution of emodin (270 mg, 1 mmol), K_2CO_3 (166 mg, 1.2 mmol) and TBAB (322 mg, 1 mmol) in DMF (22 ml) was added dropwise dibromoalkane (1.2 mmol), and the mixture was heated to 75°C for 6 hr. Distilled water was added to the mixture and it was put in a refrigerator overnight. The precipitate was filtered and washed with 5% K_2CO_3 solution to give **5a–d** as an orange solid. The crude product was purified with silica gel column, eluted with petroleum ether/CH_2Cl_2 (1:1 v/v) as eluent to afford the proposed compound.

*3-(2-Bromoethoxy)-1,8-dihydroxy-6-methylanthracene-9,10-dione (**5a**)* Orange solid, yield 50%; melting point (m.p.) 165.9–166.7°C; ^{1}H NMR (400 MHz, $CDCl_3$): δ 12.30 (s, 1H), 12.08 (s, 1H), 7.64 (s, 1H), 7.38 (s, 1H), 7.09 (s, 1H), 6.70 (s, 1H), 4.45–4.41 (t, 2H), 3.71–3.67 (t, 2H),

and 2.46 (s, 3H); ^{13}C NMR (100 MHz, $CDCl_3$) δ 190.8, 181.7, 166.0, 164.8, 162.6, 148.6, 135.4, 133.1, 124.6, 121.3, 113.6, 110.7, 108.0, 107.6, 70.1, 28.3, and 22.2; high-resolution electrospray ionization mass spectrometry (ESI-HRMS) $[M+H]^+$ *m/z* calculated for $C_{17}H_{14}BrO_5$ 377.0019, found 377.0021.

*3-(4-Bromobutoxy)-1,8-dihydroxy-6-methylanthracene-9,10-dione (**5b**)*

Orange solid, yield 65%; m.p. 136.6–137.2°C; ^{1}H NMR (400 MHz, $CDCl_3$): δ 12.29 (s, 1H), 12.11 (s, 1H), 7.62 (s, 1H), 7.33 (s, 1H), 7.06 (s, 1H), 6.65 (s, 1H), 4.14–4.12 (t, 2H), 3.52–3.49 (t, 2H), 2.44 (s, 3H), and 2.11–1.99 (m, 4H); ^{13}C NMR (100 MHz, $CDCl_3$): δ 190.7, 181.9, 166.6, 166.1, 162.6, 148.4, 135.2, 133.1, 124.5, 121.3, 113.6, 110.2, 108.4, 107.2, 67.8, 33.0, 29.7, 27.0, and 22.1; ESI-HRMS $[M+H]^+$ *m/z* calculated for $C_{19}H_{18}BrO_5$ 405.0332, found 405.0333.

*3-(5-Bromopentyloxy)-1,8-dihydroxy-6-methylanthracene-9,10-dione (**5c**)*

Orange solid, yield 68%; m.p121.7–122.9°C; ^{1}H NMR (400 MHz, $CDCl_3$): δ 12.30 (s, 1H), 12.10 (s, 1H), 7.64 (s, 1H), 7.38 (s, 1H), 7.11 (s, 1H), 6.70 (s, 1H), 4.15–4.12 (t, 2H), 3.68–3.60 (t, 2H), 2.46 (s, 3H), 2.12–1.99 (m, 4H), and 1.62–1.60 (m, 2H); ^{13}C NMR (100 MHz, $CDCl_3$): δ 190.7, 181.9, 166.9, 166.1, 162.5, 148.4, 136.2, 133.2, 124.5, 121.2, 113.6, 110.2, 108.6, 107.1, 68.0, 33.3, 32.3, 29.1, 24.7, and 22.1; ESI-HRMS $[M+H]^+$ *m/z* calculated for $C_{20}H_{20}BrO_5$ 419.0489, found 419.0491.

*3-(6-Bromohexyloxy)-1,8-dihydroxy-6-methylanthracene-9,10-dione (**5d**)*

Orange solid, yield 48%; m.p. 111.5–112.4°C; ^{1}H NMR (300 MHz, $CDCl_3$): δ 12.32 (s, 1H), 12.14 (s, 1H), 7.64 (s, 1H), 7.36 (s, 1H), 7.09 (s, 1H), 6.67 (s, 1H), 4.12–4.08 (t, 2H), 3.46–3.41 (t, 2H), 2.46 (s, 3H), 1.91–1.86 (t, 4H), and 1.58–1.56 (m, 4H); ^{13}C NMR (100 MHz, $CDCl_3$): δ 190.7, 181.9, 166.7, 166.1, 162.4, 148.5, 136.2, 133.2, 124.4, 121.3, 113.6, 110.1, 108.6, 107.2, 68.1, 33.1, 32.3, 31.8, 29.5, 24.7, and 22.3; ESI-HRMS $[M+H]^+$ *m/z* calculated for $C_{21}H_{22}BrO_5$ 433.0645, found 433.0642.

4.1.3 | General procedures for the preparation of 6a–f

A DMSO (35 ml) solution of 1,2,4-triazole or benzotriazol-1-ol (6 mmol) was slowly added to K_2CO_3 (1.1 g, 8 mmol) in DMSO (35 ml) and stirred for 1 hr at 50°C. After it cooled to room temperature, the solution of **5a–d** (5 mmol) was added dropwise to the above solution. The mixture was stirred for 8 hr at room temperature, and a yellow solution was obtained. The solvent was quenched with 20 ml water. Then, the solution was extracted with CH_2Cl_2 (5 × 20 ml), and the combined extracting solution was washed with water and then dried with anhydrous Na_2SO_4. After evaporating CH_2Cl_2 under vacuum, an orange crude product was obtained. Then, the product was purified with silica gel column and eluted with petroleum ether/dichloromethane (v/v) as eluent to afford the proposed compound.

*3-(2-(4H-1,2,4-Triazol-4-yl)ethoxy)-1,8-dihydroxy-6-methylanthracene-9,10-dione (**6a**)*

3-(2-Bromoethoxy)-1,8-dihydroxy-6-methylanthracene-9,10-dione (**5a**) was treated with 1,2,4-trizole according to the general procedure to give the desired product **6a** as an orange solid, yield 16%; m.p. 145.9–146.7°C, ^{1}H NMR (600 MHz, $CDCl_3$): δ 12.26 (s, 1H), 12.24 (s, 1H), 8.24 (s, 1H), 7.99 (s, 1H), 7.62 (s, 1H), 7.32 (d, *J* = 12 Hz, 1H), 7.08 (s, 1H), 6.64 (d, *J* = 12 Hz, 1H), 4.64 (t, *J* = 6 Hz, 2H), 4.48 (t, *J* = 12 Hz, 2H), and 2.45 (s, 3H); ^{13}C NMR (125 MHz, $CDCl_3$) δ 189.5, 178.1, 166.0, 165.0, 162.6, 159.8, 148.7, 140.5, 134.5, 127.1, 124.6, 121.4, 111.2, 110.9, 107.8, 107.5, 66.2, 48.9, and 22.1; ESI-HRMS $[M+H]^+$ *m/z* calculated for $C_{19}H_{16}N_3O_5$ 366.1084, found 366.1082.

*3-(4-(4H-1,2,4-Triazol-4-yl)butoxy)-1,8-dihydroxy-6-methylanthracene-9,10-dione (**6b**)*

3-(4-Bromo-butoxy)-1,8-dihydroxy-6-methylanthracene-9,10-dione (**5b**) was treated with 1,2,4-trizole according to the general procedure to give the desired product **6b** as an orange solid, yield 38%, m.p. 144.4–144.9°C; ^{1}H NMR (400 MHz, $CDCl_3$): δ 12.30 (s, 1H), 12.10 (s, 1H), 8.12 (s, 1H), 7.97 (s, 1H), 7.63 (s, 1H), 7.34 (d, *J* = 1.6 Hz, 1H), 7.08 (s, 1H), 6.66 (d, *J* = 2.8 Hz, 1H), 4.31–4.27 (t, *J* = 12 Hz, 2H), 4.14–4.11 (t, *J* = 10 Hz, 2H), 2.45 (s, 3H), 2.17–2.10 (m, 2 H), and 1.98–1.83 (m, 2H); ^{13}C NMR (100 MHz, $CDCl_3$): δ 190.5, 181.0, 166.0, 165.2, 162.5, 155.4, 148.4, 135.3, 130.2, 127.5, 121.2, 115.7, 110.5, 108.5, 107.5, 67.6, 49.7, 29.6, 25.4, and 22.1; ESI-HRMS $[M+H]^+$ *m/z* calculated for $C_{21}H_{20}N_3O_5$ 394.1397, found 394.1400.

*3-(6-(4H-1,2,4-Triazol-4-yl)hexyloxy)-1,8-dihydroxy-6-methylanthracene-9,10-dione (**6c**)*

3-(6-Bromo-hexyloxy)-1,8-dihydroxy-6-methylanthracene-9,10-dione (**5d**) was treated with 1,2,4-trizole according to the general procedure to give the desired product **6c** as an orange solid, yield 25%, m.p.136.2–137.1°C; ^{1}H NMR (600 MHz, $CDCl_3$): δ 12.31 (s, 1H), 12.13 (s, 1H), 8.09 (s, 1H), 7.96 (s, 1H), 7.63 (s, 1H), 7.35 (d, *J* = 6 Hz, 1H), 7.09 (s, 1H), 6.66 (d, *J* = 6 Hz, 1H), 4.22 (t, *J* = 18 Hz, 2H), 4.10 (t, *J* = 18 Hz, 2H), 2.45 (s, 3H), 1.93–1.97 (m, 2H), 1.80–1.85 (m, 2H), 1.50–1.58 (m, 2H), and 1.33–1.40 (m, 2H); ^{13}C NMR (125 MHz, $CDCl_3$) δ 190.7, 182.0, 165.9, 165.2, 162.51, 151.4, 148.4, 135.3, 133.2, 124.5, 121.2, 113.7, 110.2, 108.5, 107.1, 68.6, 49.7, 29.6, 28.6, 26.2, 25.4, and 22.1; ESI-HRMS $[M+H]^+$ *m/z* calculated for $C_{23}H_{24}N_3O_5$ 422.1710, found 422.1715.

*3-(4-(1H-Benzo[d][1,2,3]triazol-1-yloxy)butoxy)-1,8-dihydroxy-6-methylanthracene-9,10-dione (**6d**)*

3-(4-Bromo-butoxy)-1,8-dihydroxy-6-methylanthracene-9,10-dione (**5b**) was treated with 1*H*-benzo[d][1,2,3]triazol-1-ol according to the general procedure to give the desired product **6d** as an orange solid, yield 45%, m.p. 146.3–147.5°C; ^{1}H NMR (400 MHz, $CDCl_3$): δ 12.30 (s, 1H), 12.11 (s, 1H), 8.05–8.03 (d, *J* = 8.4 Hz, 1H), 7.63–7.61

(d, J = 9.6 Hz, 2H), 7.56–7.25 (t, J = 6.8 Hz, 1H), 7.43–7.39 (d, J = 8.4 Hz, 1H), 7.36–7.35 (d, J = 2.8 Hz, 1H), 7.08 (s, 1H), 6.68 (d, J = 2.8 Hz, 1H), 4.68–4.65 (t, J = 6 Hz, 2H), 4.23–4.21 (t, J = 6 Hz, 2H), 2.45 (s, 3H), 2.19–2.13 (m, 2H), and 2.13–2.09 (m, 2H); ^{13}C NMR (100 MHz, $CDCl_3$): δ 190.7, 181.8, 166.7, 166.2, 162.6, 148.5, 143.6, 136.2, 130.2, 128.1, 125.4, 124.7, 124.6, 121.3, 120.4, 113.7, 110.3, 108.6, 108.4, 107.2, 80.2, 68.2, 25.4, 24.9, and 22.1; ESI-HRMS $[M+H]^+$ m/z calculated for $C_{25}H_{22}N_3O_6$ 460.1503, found 460.1440.

*3-(5-(1H-Benzo[d][1,2,3]triazol-1-yloxy)pentalogy)-1,8-dihydroxy-6-methylanthracene-9,10-dione (**6e**)*

3-(5-Bromopentyloxy)-1,8-dihydroxy-6-methylanthracene-9,10-dione (**5c**) was treated with 1*H*-benzo[*d*][1,2,3]triazol-1-ol according to the general procedure to give the desired product **6e** as an orange solid, yield 40%, m.p. 130.1–131.8°C; ^{1}H NMR (400 MHz, $CDCl_3$): δ 12.28 (s, 1H), 12.10 (s, 1H), 8.03–8.01 (d, J = 8.4 Hz, 1H), 7.61–7.58 (d, J = 9.6 Hz, 2H), 7.55–7.51 (t, J = 8.4 Hz, 1H), 7.42–7.38 (t, J = 8 Hz, 1H), 7.34 (d, J = 2.4 Hz, 1H), 7.07 (s, 1H), 6.66 (d, J = 2.4 Hz, 1H), 4.62–4.59 (t, J = 6.4 Hz, 2H), 4.16–4.13 (t, J = 6 Hz, 2H), 2.44 (s, 3H), 2.01–1.92 (m, 4H), and 1.83–1.76 (m, 2H); ^{13}C NMR (100 MHz, $CDCl_3$): δ 190.7, 181.9, 166.8, 166.2, 162.6, 148.4, 143.6, 136.2, 130.2, 128.0, 127.3, 124.6, 124.4, 121.3, 120.3, 113.7, 110.2, 108.7, 108.5, 107.2, 80.2, 68.2, 28.6, 27.8, 22.4, and 22.1; ESI-HRMS $[M+H]^+$ m/z calculated for $C_{26}H_{24}N_3O_6$ 474.1660, found 474.1652.

*3-(6-(1H-Benzo[d][1,2,3]triazol-1-yloxy)hexyloxy)-1,8-dihydroxy-6-methylanthracene-9,10-dione (**6f**)*

3-(6-Bromohexyloxy)-1,8-dihydroxy-6-methylanthracene-9,10-dione (**5d**) was treated with 1*H*-benzo[*d*][1,2,3]triazol-1-ol according to the general procedure to give the desired product **6f** as an orange solid, yield 30%, m.p. 141.7–142.4°C; ^{1}H NMR (400 MHz, $CDCl_3$): δ 12.30 (s, 1H), 12.13 (s, 1H), 8.04–8.02 (d, J = 8.4 Hz, 1H), 7.63–7.62 (d, J = 1.2 Hz, 1H), 7.60–7.57 (d, J = 8.4 Hz, 1H), 7.54–7.51 (t, J = 6.8 Hz, 1H), 7.42–7.38 (t, J = 8 Hz, 1H), 7.36–7.35 (d, J = 2.8 Hz, 1H), 7.08 (s, 1H), 6.67 (d, J = 2.8 Hz, 1H), 4.60–4.57 (t, J = 6.4 Hz, 2H), 4.14–4.11 (t, J = 6 Hz, 2H), 2.45 (s, 3H), 1.95–1.88 (m, 4H), and 1.67–1.59 (m, 4H). ^{13}C NMR (100 MHz, $CDCl_3$): δ 190.7, 181.9, 166.7, 166.1, 162.5, 148.4, 143.7, 136.2, 130.2, 128.0, 127.4, 124.6, 124.5, 121.2, 120.3, 113.7, 110.2, 108.6, 108.4, 107.2, 80.7, 68.2, 28.7, 28.0, 26.7, 26.4, and 22.1; ESI-HRMS $[M+H]^+$ m/z calculated for $C_{27}H_{26}N_3O_6$ 488.1816, found 488.1812.

4.1.4 | General procedures for the preparation of 7a–f

An anhydrous THF (1 ml) solution of benzimidazole or imidazole (1 mmol) was slowly added to a suspension of oil-free sodium hydride (120 mg, 5 mmol) in anhydrous THF (2–3 ml) under N_2 at room temperature. When there was no gas released, an anhydrous THF (8–10 ml) solution of **5a–d** (1.5 mmol) was added dropwise to the above solution. The mixture was stirred for 3 hr at 75°C and a purple solution was obtained. The solvent was quenched with 15 ml saturated ammonium chloride aqueous solution. Then, the solution was extracted with CH_2Cl_2 (5 × 20 ml), and the combined extracting solution was washed with water and then dried with anhydrous Na_2SO_4. After evaporating CH_2Cl_2 under vacuum, an orange crude product was obtained. The crude product was filtered and washed with THF. Then, the product was purified with silica gel column, eluted with CH_2Cl_2/MeOH (150:1 v/v) as eluent to afford the proposed compound.

*3-(2-(1H-Benzo[d]imidazol-1-yl)ethoxy)-1,8-dihydroxy-6-methylanthracene-9,10-dione (**7a**)*

3-(2-Bromoethoxy)-1,8-dihydroxy-6-methylanthracene-9,10-dione (**5a**) was treated with benzimidazole according to the general procedure to give the desired product **7a** as an orange solid, yield 48%, m.p. 219.1–220.0°C; ^{1}H NMR (600 MHz, $CDCl_3$): δ 12.27 (s, 1H), 12.05 (s, 1H), 8.05 (s, 1H), 7.85 (d, J = 6.0 Hz, 1H), 7.65 (s, 1H), 7.51 (d, J = 12.0 Hz, 1H), 7.39 (t, J = 12 Hz, 1H), 7.35 (s, 1H), 7.34 (s, 1H), 7.11 (s, 1H), 6.66 (s, 1H), 4.67 (t, J = 6 Hz, 2H), 4.46 (t, J = 12 Hz, 2H), and 2.47 (s, 3H); ^{13}C NMR (125 MHz, $CDCl_3$): δ 200.8, 198.9, 181.1, 165.1, 164.7, 162.8, 148.7, 144.1, 143.2, 135.7, 133.8, 133.1, 124.9, 123.2, 122.5, 121.5, 120.8, 113.4, 110.9, 109.2, 107.7, 67.0, 43.7, and 22.4; ESI-HRMS $[M+H]^+$ m/z calculated for $C_{24}H_{19}N_2O_5$ 415.1288, found 415.1294.

*3-(4-(1H-Benzo[d]imidazol-1-yl) butoxy)-1,8-dihydroxy-6-methylanthracene-9,10-dione (**7b**)*

3-(4-Bromobutoxy)-1,8-dihydroxy-6-methylanthracene-9,10-dione (**5b**) was treated with benzimidazole according to the general procedure to give the desired product **7b** as an orange solid, yield 38%, m.p. 220.1–221.3°C; ^{1}H NMR (600 MHz, $CDCl_3$): δ 12.29 (s, 1H), 12.09 (s, 1H), 7.93 (s, 1H), 7.83 (d, J = 6 Hz, 1H), 7.63 (s, 1H), 7.43 (d, J = 6 Hz, 1H), 7.33–7.28 (m, 3H), 7.08 (s, 1H), 6.64 (d, J = 6 Hz, 1H), 4.32 (t, J = 6 Hz, 2H), 4.12 (t, J = 12 Hz, 2H), 2.45 (s, 3H), 2.12 (m, 2H), and 1.85 (m, 2H); ^{13}C NMR (125 MHz, $CDCl_3$): δ 190.9, 181.9, 165.5, 165.0, 162.7, 148.5, 144.1, 142.9, 135.3, 133.7, 133.2, 124.5, 123.0, 122.2, 121.4, 120.6, 113.8, 110.4, 109.5, 108.3, 107.2, 67.8, 44.7, 26.7, 26.3, and 22.1; ESI-HRMS $[M+H]^+$ m/z calculated for $C_{26}H_{23}N_2O_5$ 443.1601, found 443.1604.

*3-(6-(1H-Benzo[d]imidazol-1-yl)hexyloxy)-1,8-dihydroxy-6-methylanthracene-9,10-dione (**7c**)*

3-(6-Bromohexyloxy)-1,8-dihydroxy-6-methylanthracene-9,10-dione (**5d**) was treated with benzimidazole according to the general procedure to give the desired product **7c** as an orange solid, yield 35%, m.p. 223.4–224.5°C; ^{1}H NMR (600 MHz, $CDCl_3$): δ 12.30 (s, 1H), 12.12 (s, 1H), 7.91 (s, 1H), 7.82 (d, J = 6 Hz, 1H), 7.63 (s, 1H), 7.42 (d, J = 6 Hz, 1H), 7.34–7.28 (m, 3H), 7.09 (s, 1H), 6.64 (d, J = 6 Hz, 1H), 4.20 (t, J = 12 Hz, 2H), 4.08 (t, J = 12 Hz, 2H), 2.45 (s, 3H), 1.97–1.92 (m, 2H), 1.83–1.79 (m, 2H), 1.53–1.51 (m, 2H), and 1.45–1.40 (m, 2H); ^{13}C NMR (125 MHz, $CDCl_3$): δ 190.6, 181.9, 165.78, 165.0, 162.5, 148.4, 143.9, 143.0, 135.2, 133.8, 133.0, 124.2, 122.9, 122.2, 121.2, 120.6, 113.5, 110.0, 109.6, 108.5, 107.1, 68.8, 45.0, 29.8, 28.7, 26.5, 25.4, and 21.8; ESI-HRMS $[M+H]^+$ m/z calculated for $C_{28}H_{27}N_2O_5$ 471.1914, found 471.1910.

*3-(2-(1H-Imidazol-1-yl)ethoxy)-1,8-dihydroxy-6-methylanthracene-9,10-dione (**7d**)*

3-(2-Bromoethoxy)-1,8-dihydroxy-6-methylanthracene-9,10-dione (**5a**) was treated with imidazole according to the general procedure to give the desired product **7d** as an orange solid, yield 50%, m.p. 151.2–152.8°C; ^{1}H NMR (600 MHz, $CDCl_3$): δ 12.26 (s, 1H), 12.04 (s, 1H), 7.63 (s, 1H), 7.61 (s, 1H), 7.33 (d, J = 2.4 Hz, 1H), 7.10 (s, 1H), 7.08 (s, 1H), 7.06 (s, 1H), 6.65 (d, J = 1.8 Hz, 1H), 4.41–4.40 (t, J = 4.2 Hz, 2H), 4.36–4.34 (t, J = 4.2 Hz, 2H), and 2.45 (s, 3H); ^{13}C NMR (125 MH_Z, $CDCl_3$): δ 190.9, 181.7, 165.0, 164.6, 162.6, 148.7, 137.5, 135.5, 133.1, 130.0, 124.6, 121.4, 119.3, 113.6, 111.0, 107.8, 107.5, 67.9, 46.1, and 22.2; ESI-HRMS $[M+H]^+$ m/z calculated for $C_{20}H_{17}N_2O_5$ 365.1132, found 365.1124.

*3-(4-(1H-Imidazol-1-yl)butoxy)-1,8-dihydroxy-6-methylanthracene-9,10-dione (**7e**)*

3-(4-Bromoethoxy)-1,8-dihydroxy-6-methylanthracene-9,10-dione (**5b**) was treated with imidazole according to the general procedure to give the desired product **7e** as an orange solid, yield 38%, m.p. 142.7–143.9°C; ^{1}H NMR (600 MHz, $CDCl_3$): δ 12.26 (s, 1H), 12.25 (s, 1H), 7.59 (s, 1H), 7.55 (s, 1H), 7.29 (d, J = 1.8 Hz, 1H), 7.10 (s, 1H), 7.06 (s, 1H), 6.96 (s, 1H), 6.62 (d, J = 2.4 Hz, 1H), 4.10–4.08 (t, J = 5.4 Hz, 2H), 4.07–4.05 (t, J = 7.2 Hz, 2H), 2.44 (s, 3H), 2.04–2.00 (m, 2 H), and 1.86–1.81 (m, 2H); ^{13}C NMR (125 MHz, $CDCl_3$) δ 190.7, 181.9, 165.6, 165.1, 162.5, 148.5, 137.1, 135.3, 133.2, 129.6, 124.5, 121.3, 118.7, 113.6, 110.4, 108.2, 107.2, 68.0, 46.7, 27.8, 26.0, and 22.1; ESI-HRMS $[M+H]^+$ m/z calculated for $C_{22}H_{21}N_2O_5$ 393.1450, found 393.1447.

*3-(6-(1H-Imidazol-1-yl)hexyloxy)-1,8-dihydroxy-6-methylanthracene-9,10-dione (**7f**)*

3-(6-Bromohexyloxy)-1,8-dihydroxy-6-methylanthracene-9,10-dione (**5d**) was treated with imidazole according to the general procedure to give the desired product **7f** as an orange solid, yield 20%, m.p. 130.8–143.6°C; ^{1}H NMR (600 MHz, $CDCl_3$): δ 12.30 (s, 1H), 12.12 (s, 1H), 7.63 (s, 1H), 7.50 (s, 1H), 7.34 (s, 1H), 7.08 (s, 1H), 7.07 (s, 1H), 6.92 (s, 1H), 6.65 (s, 1H), 4.09–4.07 (t, J = 6.6 Hz, 2H), 3.97–3.95 (t, J = 7.2 Hz, 2H), 2.45 (s, 3H), 1.86–1.80 (m, 4H), 1.55–1.50 (m, 2H), and 1.41–1.36 (m, 2H); ^{13}C NMR (125 MHz, $CDCl_3$): δ 190.8, 182.1, 166.0, 165.2, 162.5, 148.4, 137.1, 135.3, 133.3, 129.4, 124.5, 121.3, 118.8, 113.7, 110.2, 108.5, 107.2, 68.6, 47.0, 31.0, 28.7, 26.3, 25.5, and 22.1; ESI-HRMS $[M+H]^+$ m/z calculated for $C_{24}H_{25}N_2O_5$ 421.1758, found 421.1754.

4.1.5 | Procedures for the preparation of 8a

To a solution of phenol (94 mg, 1 mmol), and K_2CO_3 (207 mg, 1.5 mmol) in DMF (2 ml) was added dropwise dibromoalkane (215 mg, 1 mmol) in DMF (8 ml), and the mixture was heated to 75°C for 24 hr and quenched with water (20 ml). The mixture was treated with water and extracted with diethyl ether (20 ml × 3). The combined organic layers were dried over $MgSO_4$ and concentrated. The crude product was purified with a silica gel column, eluted with *n*-hexane as eluent to obtain **8a** as a yellow oil. Yield 47%, ^{1}H NMR (400 MHz, $CDCl_3$): δ 7.30 (t, 2H), 6.95 (t, J = 7.3 Hz, 1H), 6.91 (t, 2H), 4.00 (t, J = 6.0 Hz, 2H), 3.50 (t, J = 6.6 Hz, 2H), 2.06 (m, 2H), and1.95 (m, 2H); ESI-HRMS $[M+H]^+$ m/z calculated for $C_{10}H_{13}BrO$ 229.0228, found 229.0233.

4.1.6 | Procedures for the preparation of 9a

An anhydrous THF (2 ml) solution of imidazole (102 mg, 1.5 mmol) was slowly added to a suspension of oil-free sodium hydride (200 mg, 8.3 mmol) in anhydrous THF (2 ml) under N_2 at room temperature for 30 min. When there was no gas released, an anhydrous THF (10 ml) solution of **8a** (229 mg, 1 mmol) was added dropwise to the above solution. The mixture was stirred for 3 hr at 60°C. The solvent was quenched with 15 ml saturated ammonium chloride aqueous solution. Then, the solution was extracted with CH_2Cl_2 (5 × 20 ml), and the combined extracting solution was washed with water, and then dried with anhydrous $MgSO_4$. After evaporating CH_2Cl_2 under vacuum, the crude product was obtained. Then, the crude product was purified with a silica gel column, eluted with CH_2Cl_2/MeOH (100:1 v/v) as eluent to afford the proposed compound **9a** as a yellow oil. Yield 74%, ^{1}H NMR (600 MHz, $CDCl_3$): δ 7.49 (s, 1H), 7.28 (t, J = 7.5 Hz, 2H), 7.06 (s, 1H), 6.95 (d, J = 7.3 Hz, 1H), 6.93 (d, J = 3.6 Hz, 1H), 6.88 (d, J = 8.0 Hz, 2H), 4.02 (t, J = 7.1 Hz, 2H), 3.97 (t, J = 6.0 Hz, 2H), 1.99 (m, 2H), and 1.78 (m, 2H). ESI-HRMS $[M+H]^+$ m/z calculated for $C_{13}H_{17}N_2$ 217.1341, found 217.1343.

4.2 | Biochemical assays

4.2.1 | Cell culture

RAW 264.7 (murine macrophage) cells were purchased from Nanjing Keygen Biotech. Co., Ltd. (Nanjing, China). The cells were maintained in a humidified atmosphere with 5% CO_2 at 37°C. The medium for cell lines was RPMI-1640, supplemented with 10% fetal bovine serum (Hangzhou Sijiqing Biological Engineering Materials Co. Ltd.), 100 IU/ml penicillin, and 100 μg/ml streptomycin (Amresco, Solon, OH). Differentiation was carried out 24 hr after the cells were seeded by adding 50 ng/ml nerve growth factor for 8 days.

4.2.2 | Nitrite measurement

RAW 264.7 mouse macrophages were plated in 96-well plates at 5×10^3/well in triplicate. On the next day, the cells were pretreated with the vehicle, indomethacin or emodin derivatives (0–20 μM dose range) for 1 hr. After a 1-hr treatment, the cells were treated with LPS (1 μg/ml) for 24 hr. NO concentration in the medium was determined using a Griess reagent kit (Beyotime, China). Control cells were cultured with equal amounts of DMSO (always <0.1% in the culture). Indomethacin was the positive control.

4.2.3 | Detection of cytokine levels in cultured supernatants

Treated cells were seeded into six-well plates. The expression levels of inflammatory cytokines, IL-1β, IL-6, and TNF-α, were measured in the supernatant using ELISA kits according to the manufacturer's protocol. The standards and samples were added to the wells. And then, a horseradish peroxidase-labeled antibody was added for 60 min at 37°C. After washing five times, the substrate was added to the wells at 37°C for 15 min and the samples were then washed another five times. Finally, the wells were treated with a stop solution. The optical density values were determined by 450 nm.

4.2.4 | Protein extraction and Western blot analysis

Proteins were prepared with RIPA lysis buffer overnight at −20°C. A bicinchoninic acid assay kit (Dingguo Biotechnology Co. Ltd., Beijing, China) was used to determine the total protein concentration. Proteins were separated by sodium dodecyl sulfate polyacrylamide gel electrophoresis and transferred onto a nitrocellulose membrane. The membranes were blocked by 5% nonfat dry milk for 2 hr and then incubated with the appropriate primary antibodies at 4°C overnight followed by incubation with the secondary antibody for an additional 1 hr at room temperature. Immunoreactivity was detected using BeyoECL Star (Beyotime Biotechnology, Shanghai, China). The expression levels of proteins were quantified with the ImageJ software (National Institutes of Health, MD).

4.2.5 | Reverse-transcription quantitative PCR (RT-qPCR) assay

High-pure total RNA was extracted using an RNA Purification Kit (BioTek, China) following the manufacturer's protocol, and was then reverse-transcribed into complementary DNA (cDNA) with an All-in-One cDNA Synthesis SuperMix (Bimake). Expression levels of COX-2, IL-1β, TNF-α, and iNOS mRNA were evaluated in triplicate by RT-qPCR using a 2× SYBR Green qPCR Master Mix (Bimake). Gene-specific primers were purchased from Sangon Biotech Co. Ltd. (Shanghai, China) and are listed in Table 2. Data from three independent experiments were analyzed, and the $2^{-\Delta\Delta C_t}$ method was used for quantification of gene expression. β-Actin was used as a house keeping gene.

4.2.6 | Cytoplasm and nucleus protein extraction

Cell lysates were added to cytoplasm extraction buffer containing phosphatase inhibitors, phenylmethylsulfonyl fluoride and dithiothreitol, then vortexed vigorously for 15 s. After incubation for 10 min on ice, the cell lysates were centrifuged at 12,000 rpm for 10 min and the cytoplasmic fraction supernatants were transferred and stored at −80°C. Nucleic proteins were fractioned using a nucleoprotein extraction kit, according to the manufacturer's instructions. Pellets were resuspended in a nuclear extraction buffer and incubated for 20 min on ice, after centrifugation at 12,000 rpm for 10 min, and the supernatant was kept as the nuclear extract and stored at −80°C until used.

TABLE 2 Real-time PCR primer pairs

Gene	Description	Primer sequence
COX-2	F	TGAGCAACTATTCCAAACCAGC
	R	GCACGTAGTCTTCGATCACTATC
iNOS	F	GTTCTCAGCCCAACAATACAAGA
	R	GTGGACGGGTCGATGTCAC
IL-6	F	TAGTCCTTCCTACCCCAATTTCC
	R	TTGGTCCTTAGCCACTCCTTC
IL-1β	F	GAAATGCCACCTTTTGACATGG
	R	TGGATGCTCTCATCAGGACAG
TNF-α	F	CAGGCGGTGCCTATGTCTC
	R	CGATCACCCCGAAGTTCAGTAG

Abbreviations: COX-2, cyclooxygenase-2; IL-6, interleukin-6; IL-1β, interleukin-1β; iNOS, inducible NO synthase; PCR, polymerase chain reaction; TNF-α, tumor necrosis factor-α.

4.2.7 | Immunofluorescence staining

RAW 264.7 cells were seeded onto confocal plates and pretreated with **7e** and indomethacin for 1 hr, and then treated with LPS (1 μg/ml) for 6 hr. After being washed three times with phosphate-buffered saline (PBS), the cells were fixed and ruptured with 4% paraformaldehyde containing 3% sucrose for 20 min. Nonfat milk (5%) in PBS was used to block cells, and primary antibodies were added to these cells overnight at 4°C; then, the cells were incubated with Alexa Fluor 488 (1:200 dilution) for 2 hr at room temperature. Besides this, the nuclei were stained with DAPI (4′,6-diamidino-2-phenylindole; 5 μg/ml) for 5 min. After being washed five times with PBS, the cells were analyzed using a confocal microscope (N-SIM E, Nikon).

ACKNOWLEDGMENTS

This project was supported by the National Natural Science Foundation of China (21602180) and the National Experimental Teaching Demonstration Center of Pharmaceutical Sciences (YX2017-CXZD-05).

CONFLICT OF INTERESTS

The authors declare that there are no conflict of interests.

ORCID

Yang Song http://orcid.org/0000-0001-7716-9216

REFERENCES

[1] X. Dong, J. Fu, X. Yin, S. Cao, X. Li, L. Lin, J. Ni, J. Ni, *Phytother. Res.* **2016**, *30*, 1207.
[2] Q. H. Ding, C. Y. Ye, E. M. Chen, W. Zhang, X. H. Wang, *Int. Immunopharmacol.* **2018**, *61*, 222.
[3] J. Li, Y. Li, X. Peng, B. Li, X. Yuan, Y. Chen, *Mol. Immunol.* **2018**, *96*, 8.
[4] Z. Liang, C. Ren, *Biomed. Pharmacother.* **2018**, *103*, 897.
[5] Y. Zheng, L. Zhu, L. Fan, W. Zhao, J. Wang, X. Hao, Y. Zhu, X. Hu, Y. Yuan, J. Shao, W. Wang, *Eur. J. Med. Chem.* **2017**, *125*, 902.
[6] X. Yang, W. Zhao, X. Hu, X. Hao, F. Hong, J. Wang, L. Xiang, Y. Zhu, Y. Yuan, R. J. Y. Ho, W. Wang, J. Shao, *Chem. Biol. Drug Des.* **2015**, *86*, 1451.
[7] S. K. Koerner, J. Hanai, S. Bai, F. E. Jernigan, M. Oki, C. Komaba, E. Shuto, V. P. Sukhatme, L. Sun, *Eur. J. Med. Chem.* **2017**, *126*, 920.
[8] J. Wu, Y. Y. Zhu, Y. H. Zhao, W. L. Shan, D. Y. Hu, J. X. Chen, D. Y. Liu, X. Y. Li, S. Yang, *Chin. Chem. Lett.* **2016**, *27*, 948.
[9] J. Wang, Y. Gan, S. Li, T. Luo, Y. Zhang, J. Zhao, *Med. Chem. Res.* **2014**, *23*, 2106.
[10] X. Zhu, X. Ye, L. Song, Y. Luo, Q. Tang, Y. Jin, X. Li, *Med. Chem. Res.* **2013**, *22*, 2228.
[11] X. Zhu, X. Ye, L. Yuan, Y. Ding, B. Zhang, X. Li, *Med. Chem. Res.* **2012**, *21*, 421.
[12] M. Park, J. Hong, *Cells* **2016**, *5*, 15.
[13] M. Karin, Y. Ben-Neriah, *Annu. Rev. Immunol.* **2000**, *18*, 621.
[14] A. Oeckinghaus, S. Ghosh, *Cold Spring Harb. Perspect. Biol.* **2009**, *1*, a000034.
[15] T. Liu, L. Zhang, D. Joo, S. C. Sun, *Signal Transduct. Target Ther.* **2017**, *2*, e17023.
[16] T. Murata, M. Shimada, S. Sakakibara, T. Yoshino, T. Masuda, T. Shintani, H. Sato, Y. Koriyama, K. Fukushima, N. Nunami, M. Yamauchi, K. Fuchikami, H. Komura, A. Watanabe, K. B. Ziegelbauer, K. B. Bacon, T. B. Lowinger, *Bioorg. Med. Chem. Lett.* **2004**, *14*, 4019.
[17] T. Murata, M. Shimada, H. Kadono, S. Sakakibara, T. Yoshino, T. Masuda, M. Shimazaki, T. Shintani, K. Fuchikami, K. B. Bacon, K. B. Ziegelbauer, T. B. Lowinger, *Bioorg. Med. Chem. Lett.* **2004**, *14*, 4013.
[18] T. Morwick, A. Berry, J. Brickwood, M. Cardozo, K. Catron, M. DeTuri, J. Emeigh, C. Homon, M. Hrapchak, S. Jacober, S. Jakes, P. Kaplita, T. A. Kelly, J. Ksiazek, M. Liuzzi, R. Magolda, C. Mao, D. Marshall, D. McNeil, A. Prokopowicz, C. Sarko, E. Scouten, C. Sledziona, S. Sun, J. Watrous, J. P. Wu, C. L. Cywin, *J. Med. Chem.* **2006**, *49*, 2898.
[19] H. Takahashi, M. Shinoyama, T. Komine, M. Nagao, M. Suzuki, H. Tsuchida, K. Katsuyama, *Bioorg. Med. Chem. Lett.* **2011**, *21*, 1758.
[20] H. Karaca gençer, U. Acar Çevik, B. Kaya Çavuşoğlu, B. N. Sağlık, S. Levent, Ö. Atlı, S. Ilgın, Y. Özkay, Z. A. Kaplancıklı, *J. Enzyme Inhib. Med. Chem.* **2017**, *32*, 732.
[21] M. N. Kumbar, R. R. Kamble, J. P. Dasappa, P. K. Bayannavar, H. A. Khamees, M. Mahendra, S. D. Joshi, S. Dodamani, V. P. Rasal, S. Jalalpure, *J. Mol. Struct.* **2018**, *1160*, 63.
[22] M. Hasan, R. K. Leak, R. E. Stratford, D. P. Zlotos, P. A. Witt-Enderby, *Pharmacol. Res. Perspect.* **2018**, *6*, e00417.
[23] A. R. Katritzky, S. Rachwal, *Chem. Rev.* **2010**, *110*, 1564.
[24] L. Jin, C. H. Zhou, *Acta Crystallogr. E* **2010**, *66*, O1264.
[25] J. C. Stoclet, B. Muller, R. Andriantsitohaina, A. Kleschyov, *Biochemistry* **1998**, *63*, 826.
[26] K. Chang, S. J. Lee, I. Cheong, T. R. Billiar, H. T. Chung, J. A. Han, Y. G. Kwon, K. S. Ha, Y. M. Kim, *Exp. Mol. Med.* **2004**, *36*, 311.
[27] J. A. Mitchell, T. W. Evans, *Inflamm. Res.* **1998**, *47*, S88.
[28] J. A. Mitchell, T. D. Warner, *Nat. Rev. Drug Discov.* **2006**, *5*, 75.

SUPPORTING INFORMATION

Additional supporting information may be found online in the Supporting Information section.

How to cite this article: Zhu X, Chen Q, Yang Y, Ai X, Chen S, Song Y. Synthesis and anti-inflammatory effects of novel emodin derivatives bearing azole moieties. *Arch Pharm Chem Life Sci.* 2019;e1900264.
https://doi.org/10.1002/ardp.201900264